How to cite: Angew. Chem. Int. Ed. 2023, e202303202
doi.org/10.1002/anie.202303202

NMR Spectroscopy

Combining Solid-State NMR with Structural and Biophysical Techniques to Design Challenging Protein-Drug Conjugates

Linda Cerofolini[+], Kristian Vasa[+], Elisa Bianconi[+], Maria Salobehaj, Giulia Cappelli, Alice Bonciani, Giulia Licciardi, Anna Pérez-Ràfols, Luis Padilla-Cortés, Sabrina Antonacci, Domenico Rizzo, Enrico Ravera, Caterina Viglianisi, Vito Calderone, Giacomo Parigi, Claudio Luchinat, Antonio Macchiarulo, Stefano Menichetti, and Marco Fragai**

Abstract: Several protein-drug conjugates are currently being used in cancer therapy. These conjugates rely on cytotoxic organic compounds that are covalently attached to the carrier proteins or that interact with them via non-covalent interactions. Human transthyretin (TTR), a physiological protein, has already been identified as a possible carrier protein for the delivery of cytotoxic drugs. Here we show the structure-guided development of a new stable cytotoxic molecule based on a known strong binder of TTR and a well-established anticancer drug. This example is used to demonstrate the importance of the integration of multiple biophysical and structural techniques, encompassing microscale thermophoresis, X-ray crystallography and NMR. In particular, we show that solid-state NMR has the ability to reveal effects caused by ligand binding which are more easily relatable to structural and dynamical alterations that impact the stability of macromolecular complexes.

Introduction

The development of a suitable drug delivery system is a crucial step in drug design to ensure extended half-lives and efficient targeting, thus achieving high therapeutic efficacy.[1,2] The conjugation of small organic drugs to protein-based biomaterials or synthetic polymers is often used to decrease renal excretion and increase their half-lives.[3] When a protein-based carrier is used, specific recognition of receptors and thus efficient targeting can be also achieved. Human serum albumin is an archetypical example of a protein used as a carrier of drugs and contrast agents.[4] It is also used as a component of nanoparticles to deliver cytotoxic molecules to cancer cells,[5,6] or fused with therapeutic peptides to prevent their fast clearance, proteolytic degradation, and to improve solubility.[7–9]

Another protein that has been considered as a drug carrier is human transthyretin (TTR hereafter), which is present in blood plasma and cerebrospinal fluid where it carries the holo-retinol binding protein and the thyroxine T_4 hormone. Functional TTR is an assembly of four identical subunits, a dimer of dimers (D_2 symmetry, total molecular mass 55 kDa). Mutations in the gene coding for TTR decrease the stability of the assembly, leading to the dissociation of the tetramer into monomers. Monomers can partially unfold and form amyloid fibrils.[10] Extracellular accumulation of TTR amyloid fibrils in different tissues and organs leads to severe disorders, and ultimately to fatal multiorgan failure. A recent therapeutic approach to treat

[*] Dr. L. Cerofolini,[+] M. Salobehaj, G. Licciardi, Dr. A. Pérez-Ràfols, L. Padilla-Cortés, S. Antonacci, Dr. D. Rizzo, Prof. Dr. E. Ravera, Prof. Dr. V. Calderone, Prof. Dr. G. Parigi, Prof. C. Luchinat, Prof. Dr. M. Fragai
Magnetic Resonance Centre (CERM), University of Florence
Via L. Sacconi 6, 50019 Sesto Fiorentino (Italy)
E-mail: fragai@cerm.unifi.it

Dr. L. Cerofolini,[+] M. Salobehaj, G. Licciardi, L. Padilla-Cortés, Dr. D. Rizzo, Prof. Dr. E. Ravera, Prof. Dr. V. Calderone, Prof. Dr. G. Parigi, Prof. C. Luchinat, Prof. Dr. M. Fragai
Consorzio Interuniversitario Risonanze Magnetiche di Metalloproteine (CIRMMP)
Via L. Sacconi 6, 50019 Sesto Fiorentino (Italy)

Dr. L. Cerofolini,[+] K. Vasa,[+] M. Salobehaj, G. Cappelli, A. Bonciani, G. Licciardi, L. Padilla-Cortés, S. Antonacci, Dr. D. Rizzo, Prof. Dr. E. Ravera, Prof. Dr. C. Viglianisi, Prof. Dr. V. Calderone, Prof. Dr. G. Parigi, Prof. C. Luchinat, Prof. S. Menichetti, Prof. Dr. M. Fragai
Department of Chemistry "Ugo Schiff", University of Florence
Via della Lastruccia 3-13, 50019 Sesto Fiorentino (Italy)
E-mail: stefano.menichetti@unifi.it

E. Bianconi,[+] Prof. Dr. A. Macchiarulo
Department of Pharmaceutical Sciences, University of Perugia
Via Fabretti n.48, 06123 Perugia (Italy)

Dr. A. Pérez-Ràfols, Prof. C. Luchinat
Giotto Biotech s.r.l, Sesto Fiorentino
Via della Madonna del Piano 6, 50019 Florence (Italy)

[+] These authors contributed equally to this work.

the familial amyloid polyneuropathy relies on small organic molecules that target thyroxine T_4 hormone binding sites.[11,12] One of these molecules, Tafamidis (2-(3,5-dichlorophenyl)benzo[*d*]oxazole-6-carboxylic acid), binds TTR at these two sites in a negative cooperative manner, but with nanomolar affinity (K_ds of ≈2 nM and ≈200 nM respectively), and prevents dissociation into monomers.[13] The high affinity of Tafamidis makes it an ideal anchor in the design of conjugates harboring hydrophobic cytotoxic drugs that would otherwise result poorly soluble. This strategy, but with a different high-affinity TTR ligand, has been already used to generate drug-protein conjugates with an improved selectivity against cancer cells.[14–16]

The rational design of protein-drug conjugates to maximize effectiveness, pharmacokinetics, and stability in vivo while minimizing their structural complexity is receiving more and more interest, and could benefit from highly accurate structural information from X-ray crystallography, NMR spectroscopy, and cryo-electron microscopy.[17–26] However, proteins that are covalently bound to, or that interact strongly with, relatively large drugs through long linkers can be difficult to crystallize. Furthermore, these systems are too big for NMR spectroscopy in solution, but still neither big nor rigid enough to allow for the use of cryo-electron microscopy.[27] Solid-state NMR may overcome these limitations, and it is already used to investigate non-crystalline protein samples, biologics and biomaterials.[28–39] Significant enhancements in sensitivity have been obtained by the recent achievements in the NMR probe technology and in biomolecular Dynamic Nuclear Polarization (DNP).[40–44]

We here report the design and synthesis of a new molecule that results from the conjugation of the cytotoxic Paclitaxel with Tafamidis (Scheme 1) to form a stable non-covalent protein-drug conjugate (PDC) with TTR. The design of this molecule starts with the combination of structural data from X-ray crystallography, and solution and solid-state NMR. Paclitaxel and Tafamidis are linked through a long PEGylated linker containing an easily hydrolysable ester bond for the release of the cytotoxic agent to its pharmacological target (Taf-Ptx hereafter, Scheme 1).

The approach used for the design of this molecule, which is aimed at maintaining a high affinity for TTR, demonstrates the strength of an integrated structural biology strategy (relying upon X-ray, solution and solid-state NMR) in the structure-based design of novel PDCs.

Results and Discussion

Tafamidis was chosen to anchor Paclitaxel to TTR due to its high affinity and because it is an approved drug with minimal side effects.[45] A relaxometry analysis was carried out to investigate the stability of the tetrameric protein and the overall steadiness of protein dynamics upon ligand binding.[30,46–48] ^{1}H NMRD profiles of 1.2 mM wild-type TTR in water solutions were acquired with and without Tafamidis (shown in Figure S1). Multiple correlation times should be considered to account for many motional processes of different water protons interacting with protein (see "NMR relaxometry measurements" in the Supporting Information).[47] The analysis of the profiles indicates the major contributions from a correlation time in agreement with the overall reorientation time expected for tetrameric TTR, as calculated with HydroNMR,[49] and from a faster correlation time of few nanoseconds. In summary, the profiles indicate that i) the reorientation time is in line with that expected for a tetrameric protein assembly, ii) there are extensive internal motions, and iii) no sizable changes in the overall dynamics of the protein occur upon ligand binding.

The X-ray structure of the Tafamidis-TTR complex (PDB code: 3TCT)[13] shows the binding mode of Tafamidis (see Figure 1 and Figure S2, S3), suggesting that functionalization of the molecule on the carboxylic acid in position 6 should not affect its interaction with TTR. Therefore, a derivative of Tafamidis bearing a six carbon atoms linker in position 6 (Compound **2**) was synthesized (see Schemes 1 and S1) as a precursor of Taf-Ptx and used to soak crystals

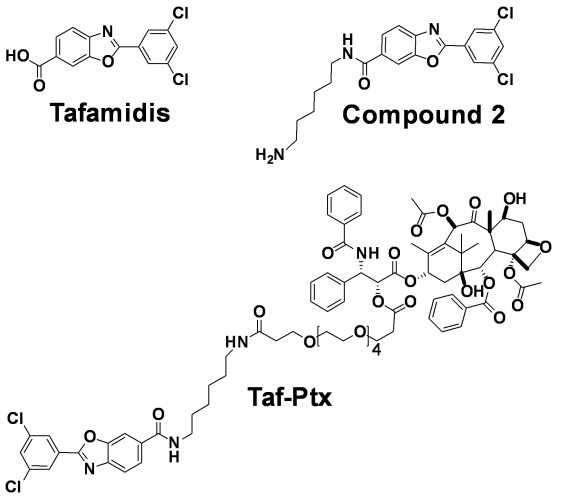

Scheme 1. Structures of Tafamidis, Compound **2**, and Taf-Ptx.

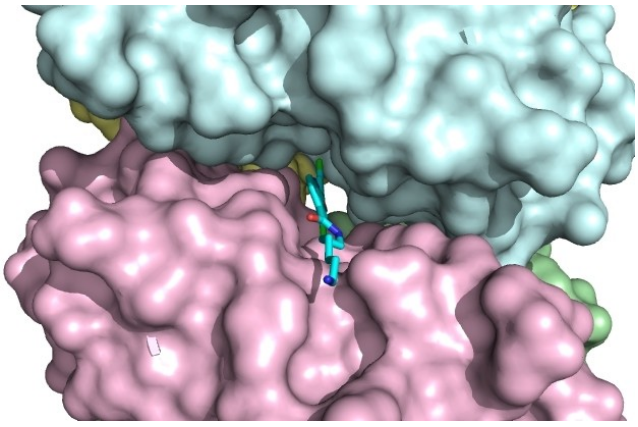

Figure 1. Detail of the surface representation of TTR interacting with compound **2** displayed as stick presented in this work (8AWW).

of TTR. The resulting X-ray structure shows that Compound **2** and Tafamidis bind TTR very similarly, and that the structure of the protein part is maintained. However, while the electron density is very well defined for all the aromatic rings in the structure of Tafamidis-bound TTR (3TCT), the Tafamidis ring that was functionalized with the hydrocarbon chain shows a weaker and less defined electron density in the structure of the adduct with Compound **2**, and this suggests a slightly higher ligand-binding heterogeneity, which in turn could be linked to a slightly lower affinity. Furthermore, the long hydrocarbon chain shows only very faint and scattered patches. This is certainly due to the mobility of this chain that is completely leaning towards the solvent. The interactions between the protein and Compound **2** are shown in Figure S4. Summarizing, the X-ray structure proves that Compound **2** preserves the binding pose of Tafamidis with the linker sticking-out from the central channel toward the solvent (see Figure 1), supporting the correct design strategy for Taf-Ptx. The X-ray structure has been deposited in the Protein Data Bank under the accession code 8AWW.

Then, the Paclitaxel molecule was conjugated to Compound **2** through an additional nineteen-atoms PEG spacer to minimize any possible steric clash with the protein and to increase the solubility. Paclitaxel is connected to the PEG spacer through an ester linkage labile in vivo,[50] which ensures its release into the cell allowing for the inhibition of tubulin polymerization.[51] As expected Taf-Ptx (Schemes 1 and S1), fails to enter the TTR crystals by soaking. Likewise, co-crystallization with TTR fails. Apparently, Taf-Ptx is too bulky, and X-ray characterization of the complex cannot be carried out. As anticipated, in cases like this, NMR could provide precious information on the structural features of the PDC, and thus validate the whole design strategy.

NMR Analysis and Assignment of Free TTR in Solution

The assignment of free tetrameric TTR in solution was obtained comparing the assignments available in the literature for the monomeric and tetrameric states of the protein,[52–55] and analyzing triple resonance spectra recorded on the perdeuterated sample of TTR. All residues (but the N-terminus, Gly-1 and Asn-98) were assigned in the spectra (Figure S5). The present assignment is the most complete and has been deposited in the bmrb under the accession code 51818.

The number of cross-peaks present in the 2D ^{1}H-^{15}N TROSY-HSQC spectrum, and the absence of signal splitting, are both consistent with the preservation of the D_2 symmetry of TTR in the tetrameric assembly. Interestingly, the signals within the same 2D spectra are characterized by different line broadening. Specifically, sharp and intense signals were observed for the residues forming loops and on the external surface of the tetramer, while broad signals were observed for the residues at the interfaces between the monomers (*i.e.*, Cys10-Lys15; His91-Phe95; Tyr105-Val121). In the 2D ^{1}H-^{15}N TROSY-HSQC spectrum recorded on the deuterated sample, these signals are also broad, suggesting the occurrence of a conformational heterogeneity/exchange for the protein (Figure S6). These features also affect the quality of the 3D ^{1}H-^{15}N NOESY spectrum, where only few NOE correlations are visible (Figure S7). As expected for a folded protein of 55 kDa, in the 2D ^{13}C-^{15}N CON spectrum only signals of the flexible regions, which are not well-defined in most X-ray structures, can be observed (Thr3-Cy10; Ala37-Thr40; Glu51-Ser52; Asn124-Glu127; see Figure S8).

NMR Analysis and Assignment of Free TTR in the Solid-State

The solid-state NMR spectra of re-hydrated freeze-dried tetrameric TTR are of good quality and characterized by a good signal resolution (Figure S9). Nevertheless, around 20 % of the expected resonances are missing and some signals are characterized by large line-broadening. Assignment of the free tetrameric protein was also obtained in the solid-state (Figure S10). The available assignment of the free protein in solution was used as starting point and complemented by the analysis of carbon-detected spectra acquired in the solid-state. The residues whose signals are missing in the spectra are mainly located at the N-terminus (up to Lys15) and in flexible regions: Asp38-Thr40, Gly57-Leu58, Phe64, Ser117-Thr119, Thr123-Asn124, Lys126. Nevertheless, as much as 80 % of the spin systems of the protein could be reassigned in the solid-state NMR spectra.

NMR Analysis and Assignment of TTR-Tafamidis and TTR-Taf-Ptx in Solution

The binding-mode of Tafamidis to [U-^{13}C, ^{15}N] TTR was first analyzed by solution NMR. During the NMR titration, the cross-peaks of the free protein in the 2D ^{1}H-^{15}N TROSY-HSQC spectra decrease in intensity upon the addition of increasing concentrations of the ligand, while new cross-peaks, corresponding to the complex between TTR and Tafamidis, appear and increase in intensity. This behavior indicates that the ligand is in slow exchange regime on the NMR timescale, and confirms its expected high affinity towards the protein.[13,56] In the presence of Tafamidis at 100 μM concentration (ligand:tetramer ratio equal to 0.5:1) the cross-peaks corresponding to the free protein and to the protein bound to the ligand have similar intensities (Figure S11A), as it can be seen for the signal of Ser112 located at the interface between the dimers of the tetrameric assembly (PDB code: 3TCT).[13] During the titration the quality of spectra decreases up to a 1:1 ligand:tetramer ratio; some signals are broadened and some disappeared. The signal's line-width sharpens again at 2:1 ligand:tetramer ratio (Figure S12), in line with the lower affinity for the second binding event. The analysis of the chemical shift perturbation (CSP) was thus performed with a ligand in slight excess with respect to the 2:1 ratio. Figure S12 confirmed that the residues experiencing the largest changes (Lys15, Leu17, Ala19, Val20, Arg21, Gly22, Ser23, Ile26, Gly53, His88, Val94, Tyr105, Thr106, Ile107, Leu111,

Ser112, Ala120, Val122) are in the expected Tafamidis binding site (Figure S13). Some of the signals experiencing large perturbations (Ala19, Arg21, Gly22, Leu111) have been tentatively reassigned with some uncertainty (Figure S13A). Interestingly, the signals corresponding to residue Ser117 and Thr118, which are almost missing in the spectra of the free protein, appear with increased intensity in the spectrum of TTR in the presence of Tafamidis. This last observation is consistent with Tafamidis stabilizing the protein tetramer.

NMR titration in solution was also performed with the newly designed ligand, Taf-Ptx. The evolution of the spectra upon addition of increasing amounts of Taf-Ptx was superimposable to that previously observed for Tafamidis, with several protein resonances experiencing a slow exchange regime on the NMR timescale. After the addition of Taf-Ptx, in the presence of a ligand:tetramer ratio equal to 0.5:1, the signals of the free protein and those of the protein bound to the ligand have similar intensities (Figure S11B). As with Tafamidis, some protein signals broaden/disappear at 1:1 ligand:tetramer ratio and sharpen/reappear again in the 2:1 complex (Figure S12C and D). The analysis of CSP of the protein signals in the 2:1 complex (Figure S13B) confirmed that the residues experiencing the largest changes (Lys15, Val20, Arg21, Gly22, Ala25, Leu111, Ser112, Ala120, Val122) are in the same protein region affected by the presence of Tafamidis (Figure S13D). It is important to point out that the signals of some residues mostly affected by CSP in the spectrum of Tafamidis-TTR (Ala19, His88, Val94, Tyr105, T106) are broadened beyond detection in the spectrum of Taf-Ptx-TTR. This is probably related to the previously described slightly higher ligand-binding heterogeneity of Taf-Ptx-TTR with respect to that of Tafamidis-TTR.

NMR Analysis and Assignment of Tafamidis-TTR and Taf-Ptx-TTR in the Solid-State

Further interesting features of the complexes between TTR and Tafamidis or Taf-Ptx are revealed by solid-state NMR. The 2D solid-state NMR spectra of these complexes exhibit a higher number of cross-peaks with respect to those of the free protein. Specifically, in the 2D ^{13}C-^{13}C dipolar-assisted rotational resonance (DARR) spectrum of TTR in the presence of either Tafamidis or Taf-Ptx, several new signals appear or increase in intensity (Gly57, Arg103, Ile107, Ala108, Ser117, Thr118, Thr119, Ala120, Thr123; see Figure 2, panel A and B). This also occurs for a few signals in the 2D ^{15}N-^{13}C NCA spectra (Figure 3A and B). These signals belong to residues located at the tetramer interface, where Tafamidis binds (Figure 3, panels E and F). The increase in signal intensity can be explained by a higher rigidity of this region after the binding of Tafamidis, which is known to stabilize the tetrameric form of the protein. As shown by the high similarity of the spectra of TTR bound to one ligand or to the other, the high affinity of Tafamidis, and its stabilizing effect on the tetramer, are still present also when the Tafamidis unit is conjugated to the Paclitaxel unit. A lower intensity of the signals corresponding to only residues S117 and T118 is observed when TTR binds to Taf-Ptx compared to when it binds to Tafamidis.

The analysis of the CSP of TTR bound to Tafamidis or Taf-Ptx with respect to the free protein indicates that the signals influenced by the ligands are largely the same. Most of the signals experiencing the largest perturbations correspond to residues at the dimer/tetramer interface (Figure 3).

To rule out the possibility that the differences, observed in the analysis of CSPs performed for solution and solid-state NMR data, are due to the comparison of different nuclei (*i.e.* ^{1}H and ^{15}N in solution, and $^{13}C\alpha$ and ^{15}N in the solid-state), the ^{15}N chemical shifts were separately compared. The analysis confirms that the largest perturbations are observed in the same areas (Figure S14).

Microscale Thermophoresis for Ligand Binding Assay

The interaction between TTR and Taf-Ptx was analyzed using a ligand binding assay with microscale thermophoresis (MST). MST detects the migration of a macromolecule in a temperature gradient, which strongly depends on size, charge, conformation and hydration shell parameters of the macromolecule. Upon a ligand binding event to the macromolecule, at least one of these parameters change, resulting in a different thermophoretic behavior.[57] In the MST experiment, 16 capillary tubes are prepared containing a fluorescent labelled protein at constant concentration and a serial titration of unlabeled ligand. An infrared laser is used to generate a temperature gradient in each tube and induce migration of the ligand-bound complex, whose fluorescence is monitored in real time. Fluorescence variations are then used to generate a binding curve as a function of ligand concentration, which is instrumental to derive the dissociation constant (K_d).[58]

MST binding experiments were performed adding Taf-Ptx to fluorescently labelled TTR (RED-TTR). A biphasic binding curve was observed, suggesting the presence of more than one Taf-Ptx binding site on RED-TTR (Figure S15A). Specifically, at low concentrations of Taf-Ptx, a first binding event is observed with the occupancy of a high affinity site by Taf-Ptx in the target protein. Then, at higher ligand concentrations, a second binding event occurs with the occupancy of a low affinity binding site. These two binding events are well separated by approximately three orders of magnitude and thus can be independently analyzed with good approximation to obtain the relative dissociation constants ($K_d1 = 0.065 \pm 0.017$ μM, Figure S15C; $K_d2 = 9.21 \pm 1.14$ μM, Figure S15B). The second dissociation constant is found lower than the first for Taf-Ptx as for Tafamidis alone, and this is consistent with the NMR observations.

Overall, these results are in agreement with the NMR measurements and with literature data,[13] supporting a high affinity interaction between Taf-Ptx and TTR with a conjugated ligand/protein stoichiometry of 2:1.

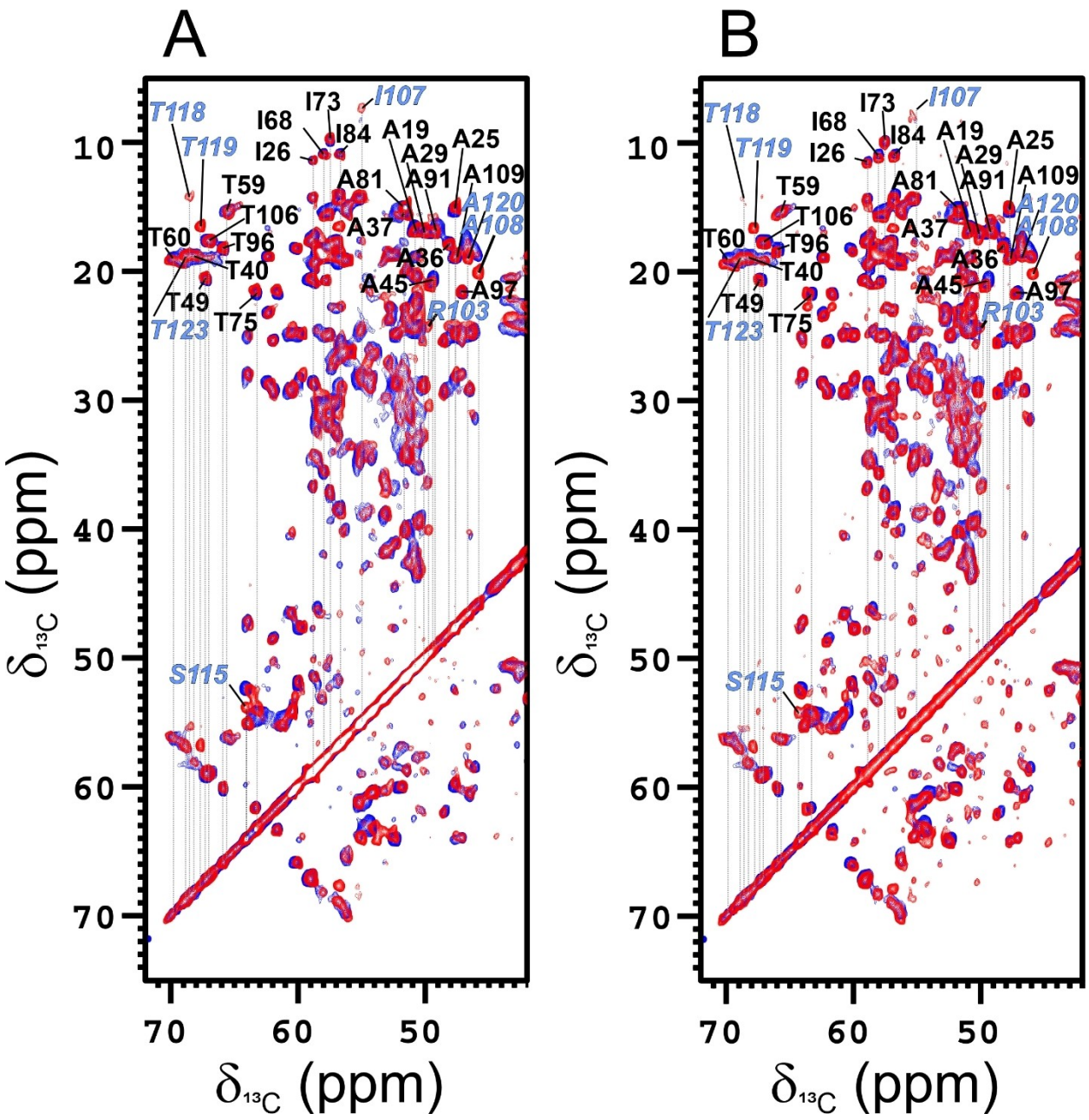

Figure 2. Comparison of a region of 2D ^{13}C-^{13}C DARR spectra (mixing time 50 ms, A, B) of free rehydrated freeze-dried TTR (blue) and TTR in the presence of the ligands (red), Tafamidis (A) or Taf-Ptx (B). The assignment of the cross-peaks related to correlations of Cβ/Cγ2 in threonine, Cα/Cδ1 in isoleucine and Cα/Cβ in alanine has been reported in the spectra. The signals with increased intensity in the spectra of TTR in complex with the ligands with respect to the free protein, have been labeled in italic font and colored in cyan. Assignment is reported also for the cross-peaks between Cβ/Cα of serine 115 and Cα/Cβ of arginine 103.

Chemical Denaturation Assay for Evaluating Taf-Ptx-Induced Stability of TTR

The impact of Taf-Ptx binding to TTR on the stability of the tetrameric protein was then evaluated using a chemical denaturation assay. Specifically, the intrinsic fluorescence of tryptophan residues (Trp41, Trp79) was monitored while denaturing the protein assembly with increasing concentrations of urea in the absence and presence of Taf-Ptx (see *Chemical denaturation assay* section in Supporting Information). In the presence of 50 μM Taf-Ptx, the tetrameric protein complex gains stability, with the relative denaturation curve shifting rightward and not reaching an unfolding plateau (Figure S16). A ΔG value $>47.3\pm2.5$ kJ mol^{-1} can be estimated in this case, suggesting a significant Taf-Ptx induced stability of TTR complex (Table S3).

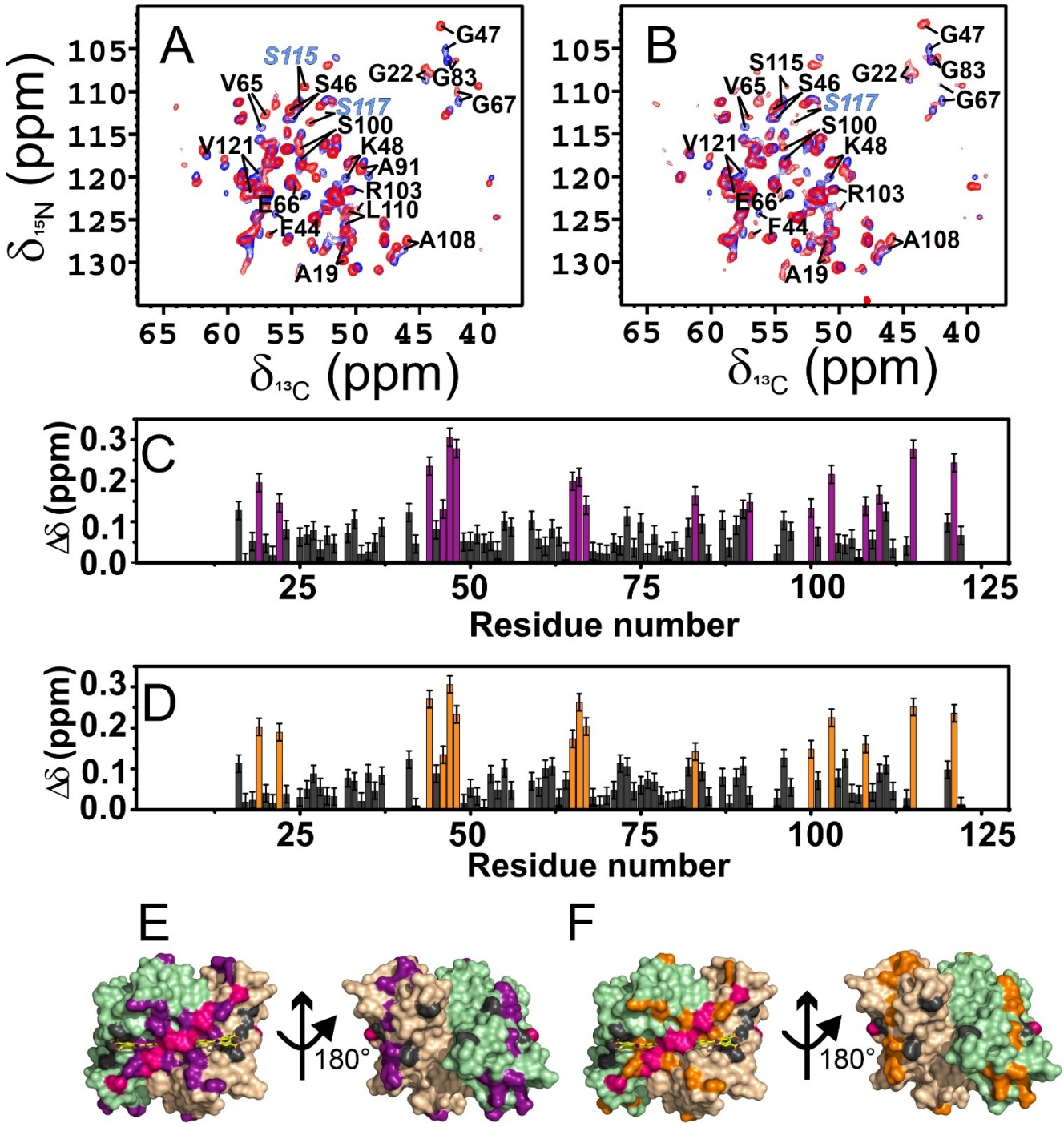

Figure 3. A), B) 2D ^{15}N ^{13}C NCA spectra of free rehydrated freeze-dried TTR (blue) and TTR in the presence of the ligands (red), Tafamidis (A) or Taf-Ptx (B). Assignment has been reported for the cross-peaks experiencing the largest perturbations ($\Delta\delta \geq$ mean + std. dev.). The signals with increased intensity in the spectra of TTR in complex with the ligands with respect to the free protein, have been labeled in italic font and colored in cyan. C), D) Chemical shift perturbation (CSP) of rehydrated freeze-dried TTR in the presence of Tafamidis (C) and Taf-Ptx (D) with respect to free rehydrated freeze-dried TTR, evaluated according to the formula $\Delta\delta = {}^1/_2\sqrt{(\Delta\delta_{C_\alpha}/2)^2 + (\Delta\delta_N/5)^2}$.[59] The residues experiencing the largest variations have been highlighted in violet (Ala19, Gly22, Phe44, Ser46, Gly47, Lys48, Val65, Glu66, Gly67, Gly83, Ala91, S100, Arg103, Ala108, Leu110, Ser115, Val121, for Tafamidis) and orange (Ala19, Gly22, Phe44, Ser46, Gly47, Lys48, Val65, Glu66, Gly67, Gly83, Ser100, Arg103, Ala108, Ser115, Val121, for Taf-Ptx), respectively. The error for CSP has been evaluated considering the standard deviation of the values of CSP below the mean, calculated considering all the CSP values. E), F) CSP mapping on the X-ray structure of TTR in complex with Tafamidis (PDB code: 3TCT)[13] with the residues experiencing the largest CSP in the presence of Tafamidis or Taf-Ptx colored in violet (E) and orange (F), respectively. The residues experiencing an increase in signal intensity after Tafamidis or Taf-Ptx binding have been colored in magenta. The residues missing in solid-state spectra are colored in grey. The monomers are in different colors (wheat, green) and Tafamidis is shown as yellow sticks.

Conclusion

CSP in solution are extensively used to analyze and compare the binding mode of ligands interacting with proteins or nucleic acids. For TTR the spectral changes resulting from the binding of Tafamidis or Taf-Ptx clearly point to a slow exchange regime on the NMR time scale for both ligands. Most of the residues experiencing the largest chemical shift variations on the NH resonances are placed at the interface of the two dimers and form the central channel hosting the thyroxine T4 hormone. Specifically, Lys15, Val20, Arg21, Gly22, Leu111, Ser112, Ala120, Val122 show chemical shift perturbations in the presence of both ligands, Tafamidis and Taf-Ptx. More importantly, the analysis of the X-ray structure (3TCT) of the 2:1 Tafamidis-TTR complex reveals that only Lys15, Leu17, and Thr106 appear to interact directly with the two ligand molecules among the residues experiencing the largest CSP. Therefore, the largest chemical shift perturbations appear to be mostly determined by the structural rearrangement induced by the two ligand molecules, making chemical shift mapping for the identification of the binding mode extremely challenging.

The stabilizing effect of Tafamidis was unambiguously proven in vitro and in vivo.[13,45] However, the chemical shift mapping obtained by NMR in solution provides only indirect evidence of this important structural effect, which can be inferred from the slow exchange regime on the NMR timescale of the signals corresponding to the residues where the binding occurs. In this respect, the observation of the slightly better quality of the spectra recorded on TTR in the presence of Tafamidis and Taf-Ptx is more informative.

It is important to point out that the use of solid-state NMR is critical for achieving a complete picture about the structural and dynamical features of this system. Indeed, the analysis of the data recorded on the solid-state samples of TTR in the presence and in the absence of the two ligands provides information that is out of reach for both X-ray crystallography and solution NMR. The comparative analyses on Tafamidis and Taf-Ptx were carried out using ^{15}N-^{13}C isotopically enriched samples of TTR and ^{13}C-detected experiments. The analysis of the NCA spectra shows that TTR in complex with Tafamidis and Taf-Ptx exhibits the largest chemical shift variations on the same residues, with very few differences. This constitutes further experimental evidence of the very similar binding mode of Taf-Ptx and Tafamidis. The chemical shift variations affect several residues placed at the interface of the two dimers around the central channel as previously observed by NMR in solution. Four of these residues (Ala108, Leu110, Ser115 and Val121) are near the ligands in the X-ray structure 3TCT. The non-overlap between solution and solid-state data about the residues experiencing the largest effects is probably due to a slightly higher conformational heterogeneity of the ligand-protein complex in solution, although in both cases they are localized at the interface between the two dimers forming the assembly. This can be clearly inferred from Figure 4, where the residues experiencing the largest CSPs ($\Delta\delta \geq$ mean + std. dev.) in solution and in the solid-state are shown together.

NMRD measurements indicate that the tetrameric assembly of TTR is maintained, and possibly reinforced, in the presence of Tafamidis. However, relaxometry is not sensitive to the presence of multiple conformational states with similar reorientation time. Important information on this respect was obtained from the qualitative analysis of the signal intensity on DARR and NCA spectra. Figure 4C shows that several residues placed at the interface between the two dimers forming the assembly, including some also experiencing large chemical shift variation, increase in intensity or appear in the spectra in the presence of Tafamidis and Taf-Ptx. The increase in signal intensity or the appearance of a signal previously undetectable in the solid-state spectra is conclusive evidence of an equilibrium of the residue shifting toward a unique conformation. This is associated with the structural stabilization of the tetrameric assembly, here proven by the chemical denaturation assay, resulting from the interaction with two high affinity ligand molecules with TTR. Therefore, the analysis provides a map of the residues experiencing a decrease of the conformational heterogeneity, thus providing a different and more informative parameter to monitor the binding mode and to evaluate the effects of the interaction with the ligands. This

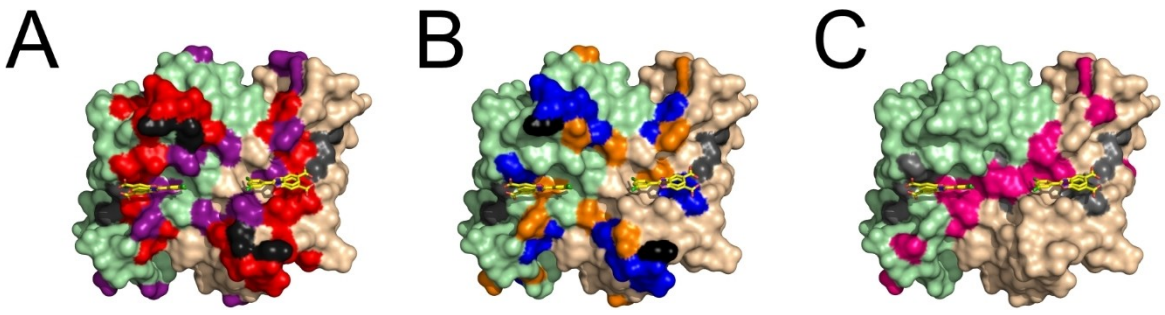

Figure 4. Comparative analysis of the NMR data collected in solution and in the solid-state of the effects of Tafamidis (A) and Taf-Ptx (B) on TTR. The residues experiencing in solution the largest CSP ($\Delta\delta \geq$ mean + std. dev.) in the presence of Tafamidis or Taf-Ptx are colored in red (A) or blue (B), respectively. The residues experiencing in the solid-state the largest CSP in the presence of Tafamidis or Taf-Ptx are colored in violet (A) or orange (B), respectively. Residues experiencing the largest CSP both in solution and in the solid state are reported in black. C) Residues experiencing in the solid-state an increase in signal intensity after the binding of Tafamidis or Taf-Ptx are colored in magenta. The residues missing in solid-state spectra are colored in grey. Monomers are in different colors (wheat, green) and Tafamidis is shown as yellow sticks.

information cannot be immediately inferred from the analysis of the CSP or from the observed improved quality of the NMR spectra recorded in solution.

When feasible, the integration of different structural biophysical methodologies is obviously the best option to develop PDCs. However, solid-state NMR can also be used on its own when the features of the investigated system prevent the use of other structural methodologies. The quality of the spectra obtained from the rehydrated freeze-dried samples, the high sensitivity of solid-state NMR to the effects of ligand binding and to small conformational heterogeneities make this technique extremely helpful to characterize the interaction of drug candidates with large monomeric/multimeric carrier proteins. In this regard, the information obtained from solid-state NMR data can be particularly important also for systems amenable to NMR characterization in solution, when the traditional chemical shift mapping based on the analysis of CSPs is not informative or resolutive.

Acknowledgements

This work has been supported by Regione Toscana (CERM-TT, BioEnable, and PANCREAS-AD bando salute 2018), the JOYNLAB laboratory, the Italian "Progetto Dipartimenti di Eccellenza 2023-2027 (DICUS2.0)". The authors acknowledge the support and the use of resources of Instruct-ERIC, a landmark ESFRI project, and specifically the CERM/CIRMMP Italy centre. We acknowledge H2020 projects INFRAIA iNEXT-Discovery (contract n° 871037), FET-Open HIRES-MULTIDYN (contract n° 899683), PANACEA (contract n° 101008500), the Marie Sklodowska-Curie Action (MSCA) Innovative Training Networks (ITN) "RNAct" H2020-MSCA-ITN-2018 (contract n° 813239) and MSCA-ITN "Glytunes" (contract n° 956758), Fragment Screen (contract n° 101094131), and the project "Potentiating the Italian Capacity for Structural Biology Services in Instruct Eric (ITACA.SB)" (Project n° IR0000009) within the call MUR 3264/2021 PNRR M4/C2/L3.1.1, funded by the European Union NextGenerationEU. Authors AM and EB acknowledge research support by the European Union - NextGenerationEU under the Italian Ministry of University and Research (MUR) National Innovation Ecosystem grant ECS00000041–VITALITY, and Università degli Studi di Perugia and MUR for support within the project Vitality.

Conflict of Interest

The authors declare no conflict of interest.

Data Availability Statement

The data that support the findings of this study are openly available in Protein Data Bank https://www.rcsb.org/ and Biological Magnetic Resonance Bank https://bmrb.io/. The raw data of the SSNMR spectra are available at https://zenodo.org under the DOI: 10.5281/zenodo.8020132.

Keywords: Drug Delivery · Drug Design · NMR Spectroscopy · Protein-Drug Conjugates · Structural Biology

[1] P. Akkapeddi, S.-A. Azizi, A. M. Freedy, P. M. S. D. Cal, P. M. P. Gois, G. J. L. Bernardes, *Chem. Sci.* **2016**, *7*, 2954–2963.
[2] R. V. J. Chari, M. L. Miller, W. C. Widdison, *Angew. Chem. Int. Ed.* **2014**, *53*, 3796–3827.
[3] J. M. Harris, R. B. Chess, *Nat. Rev. Drug Discovery* **2003**, *2*, 214–221.
[4] P. Caravan, N. J. Cloutier, M. T. Greenfield, S. A. McDermid, S. U. Dunham, J. W. M. Bulte, J. C. Amedio, R. J. Looby, R. M. Supkowski, W. D. Horrocks, T. J. McMurry, R. B. Lauffer, *J. Am. Chem. Soc.* **2002**, *124*, 3152–3162.
[5] J. Huang, B. Wu, Z. Zhou, S. Hu, H. Xu, Y. Piao, H. Zheng, J. Tang, X. Liu, Y. Shen, *Nanomedicine: Nanotechnol. Biol. Med.* **2019**, *21*, 102058.
[6] O. A. Mandrup, S. C. Ong, S. Lykkemark, A. Dinesen, I. Rudnik-Jansen, N. F. Dagnæs-Hansen, J. T. Andersen, L. Alvarez-Vallina, K. A. Howard, *Commun. Biol.* **2021**, *4*, 310.
[7] A. Zorzi, S. Linciano, A. Angelini, *MedChemComm* **2019**, *10*, 1068–1081.
[8] A. Spada, J. Emami, J. A. Tuszynski, A. Lavasanifar, *Mol. Pharmaceutics* **2021**, *18*, 1862–1894.
[9] A. D. AlQahtani, D. O'Connor, A. Domling, S. K. Goda, *Biomed. Pharmacother.* **2019**, *113*, 108750.
[10] A. W. Yee, M. Aldeghi, M. P. Blakeley, A. Ostermann, P. J. Mas, M. Moulin, D. de Sanctis, M. W. Bowler, C. Mueller-Dieckmann, E. P. Mitchell, M. Haertlein, B. L. de Groot, E. Boeri Erba, V. T. Forsyth, *Nat. Commun.* **2019**, *10*, 925.
[11] M. M. Alhamadsheh, S. Connelly, A. Cho, N. Reixach, E. T. Powers, D. W. Pan, I. A. Wilson, J. W. Kelly, I. A. Graef, *Sci. Transl. Med.* **2011**, *3*, 97ra81.
[12] M. Miller, A. Pal, W. Albusairi, H. Joo, B. Pappas, M. T. Haque Tuhin, D. Liang, R. Jampala, F. Liu, J. Khan, M. Faaij, M. Park, W. Chan, I. Graef, R. Zamboni, N. Kumar, J. Fox, U. Sinha, M. Alhamadsheh, *J. Med. Chem.* **2018**, *61*, 7862–7876.
[13] C. E. Bulawa, S. Connelly, M. DeVit, L. Wang, C. Weigel, J. A. Fleming, J. Packman, E. T. Powers, R. L. Wiseman, T. R. Foss, I. A. Wilson, J. W. Kelly, R. Labaudinière, *Proc. Natl. Acad. Sci. USA* **2012**, *109*, 9629–9634.
[14] A. Pal, W. Albusairi, F. Liu, M. T. H. Tuhin, M. Miller, D. Liang, H. Joo, T. U. Amin, E. A. Wilson, J. S. Faridi, M. Park, M. M. Alhamadsheh, *Mol. Pharmaceutics* **2019**, *16*, 3237–3252.
[15] S. C. Penchala, M. R. Miller, A. Pal, J. Dong, N. R. Madadi, J. Xie, H. Joo, J. Tsai, P. Batoon, V. Samoshin, A. Franz, T. Cox, J. Miles, W. K. Chan, M. S. Park, M. M. Alhamadsheh, *Nat. Chem. Biol.* **2015**, *11*, 793–798.
[16] F. Liu, T. Ul Amin, D. Liang, M. S. Park, M. M. Alhamadsheh, *J. Med. Chem.* **2021**, *64*, 14876–14886.
[17] J.-P. Renaud, A. Chari, C. Ciferri, W. Liu, H.-W. Rémigy, H. Stark, C. Wiesmann, *Nat. Rev. Drug Discovery* **2018**, *17*, 471–492.
[18] J. M. Lamley, D. Iuga, C. Öster, H.-J. Sass, M. Rogowski, A. Oss, J. Past, A. Reinhold, S. Grzesiek, A. Samoson, J. R. Lewandowski, *J. Am. Chem. Soc.* **2014**, *136*, 16800–16806.
[19] A. Mainz, T. L. Religa, R. Sprangers, R. Linser, L. E. Kay, B. Reif, *Angew. Chem. Int. Ed.* **2013**, *52*, 8746–8751.
[20] A. Mainz, S. Jehle, B. J. van Rossum, H. Oschkinat, B. Reif, *J. Am. Chem. Soc.* **2009**, *131*, 15968–15969.
[21] U. B. le Paige, S. Xiang, M. M. R. M. Hendrix, Y. Zhang, G. E. Folkers, M. Weingarth, A. M. J. J. Bonvin, T. G. Kutateladze,

I. K. Voets, M. Baldus, H. van Ingen, *Magn. Reson.* **2021**, *2*, 187–202.
[22] L. Eshun-Wilson, R. Zhang, D. Portran, M. V. Nachury, D. B. Toso, T. Löhr, M. Vendruscolo, M. Bonomi, J. S. Fraser, E. Nogales, *Proc. Natl. Acad. Sci. USA* **2019**, *116*, 10366–10371.
[23] H. Kato, H. van Ingen, B.-R. Zhou, H. Feng, M. Bustin, L. E. Kay, Y. Bai, *Proc. Natl. Acad. Sci. USA* **2011**, *108*, 12283–12288.
[24] A. M. Gronenborn, D. R. Filpula, N. Z. Essig, A. Achari, M. Whitlow, P. T. Wingfield, G. M. Clore, *Science* **1991**, *253*, 657–661.
[25] E. Barbet-Massin, C.-T. Huang, V. Daebel, S.-T. D. Hsu, B. Reif, *Angew. Chem. Int. Ed.* **2015**, *54*, 4367–4369.
[26] D. Rizzo, L. Cerofolini, S. Giuntini, L. Iozzino, C. Pergola, F. Sacco, A. Palmese, E. Ravera, C. Luchinat, F. Baroni, M. Fragai, *J. Am. Chem. Soc.* **2022**, *144*, 10006–10016.
[27] Q. Wang, H. Yang, X. Liu, L. Dai, T. Ma, J. Qi, G. Wong, R. Peng, S. Liu, J. Li, S. Li, J. Song, J. Liu, J. He, H. Yuan, Y. Xiong, Y. Liao, J. Li, J. Yang, Z. Tong, B. D. Griffin, Y. Bi, M. Liang, X. Xu, C. Qin, G. Cheng, X. Zhang, P. Wang, X. Qiu, G. Kobinger, Y. Shi, J. Yan, G. F. Gao, *Sci. Transl. Med.* **2016**, *8*, 369ra179.
[28] S. Giuntini, L. Cerofolini, E. Ravera, M. Fragai, C. Luchinat, *Sci. Rep.* **2017**, *7*, 17934.
[29] L. Cerofolini, S. Giuntini, E. Ravera, C. Luchinat, F. Berti, M. Fragai, *npj Vaccines* **2019**, *4*, 20.
[30] L. Cerofolini, S. Giuntini, A. Carlon, E. Ravera, V. Calderone, M. Fragai, G. Parigi, C. Luchinat, *Chem. Eur. J.* **2019**, *25*, 1984–1991.
[31] E. Ravera, S. Ciambellotti, L. Cerofolini, T. Martelli, T. Kozyreva, C. Bernacchioni, S. Giuntini, M. Fragai, P. Turano, C. Luchinat, *Angew. Chem. Int. Ed.* **2016**, *55*, 2446–2449.
[32] L. Lecoq, M.-L. Fogeron, B. H. Meier, M. Nassal, A. Böckmann, *Viruses* **2020**, *12*, E1069.
[33] T. Wiegand, D. Lacabanne, A. Torosyan, J. Boudet, R. Cadalbert, F. H.-T. Allain, B. H. Meier, A. Böckmann, *Front. Mol. Biosci.* **2020**, *7*, 17.
[34] M. Lu, R. W. Russell, A. J. Bryer, C. M. Quinn, G. Hou, H. Zhang, C. D. Schwieters, J. R. Perilla, A. M. Gronenborn, T. Polenova, *Nat. Struct. Mol. Biol.* **2020**, *27*, 863–869.
[35] M. T. Eddy, T.-Y. Yu, G. Wagner, R. G. Griffin, *J. Biomol. NMR* **2019**, *73*, 451–460.
[36] M. Fragai, C. Luchinat, T. Martelli, E. Ravera, I. Sagi, I. Solomonov, Y. Udi, *Chem. Commun.* **2014**, *50*, 421–423.
[37] K. Jaudzems, A. Kirsteina, T. Schubeis, G. Casano, O. Ouari, J. Bogans, A. Kazaks, K. Tars, A. Lesage, G. Pintacuda, *Angew. Chem. Int. Ed.* **2021**, *60*, 12847–12851.
[38] D. Rizzo, L. Cerofolini, A. Pérez-Ràfols, S. Giuntini, F. Baroni, E. Ravera, C. Luchinat, M. Fragai, *Anal. Chem.* **2021**, *93*, 11208–11214.
[39] S. Gupta, R. Tycko, *J. Biomol. NMR* **2018**, *70*, 103–114.
[40] R. Gupta, H. Zhang, M. Lu, G. Hou, M. Caporini, M. Rosay, W. Maas, J. Struppe, J. Ahn, I.-J. L. Byeon, H. Oschkinat, K. Jaudzems, E. Barbet-Massin, L. Emsley, G. Pintacuda, A. Lesage, A. M. Gronenborn, T. Polenova, *J. Phys. Chem. B* **2019**, *123*, 5048–5058.
[41] T. Azaïs, S. Von Euw, W. Ajili, S. Auzoux-Bordenave, P. Bertani, D. Gajan, L. Emsley, N. Nassif, A. Lesage, *Solid State Nucl. Magn. Reson.* **2019**, *102*, 2–11.
[42] J. Viger-Gravel, F. M. Paruzzo, C. Cazaux, R. Jabbour, A. Leleu, F. Canini, P. Florian, F. Ronzon, D. Gajan, A. Lesage, *Chem. Eur. J.* **2020**, *26*, 8976–8982.
[43] A. Hassan, C. M. Quinn, J. Struppe, I. V. Sergeyev, C. Zhang, C. Guo, B. Runge, T. Theint, H. H. Dao, C. P. Jaroniec, M. Berbon, A. Lends, B. Habenstein, A. Loquet, R. Kuemmerle, B. Perrone, A. M. Gronenborn, T. Polenova, *J. Magn. Reson.* **2020**, *311*, 106680.
[44] R. Zhang, Y. Hong, T. Ravula, Y. Nishiyama, A. Ramamoorthy, *J. Magn. Reson.* **2020**, *313*, 106717.
[45] M. S. Maurer, J. H. Schwartz, B. Gundapaneni, P. M. Elliott, G. Merlini, M. Waddington-Cruz, A. V. Kristen, M. Grogan, R. Witteles, T. Damy, B. M. Drachman, S. J. Shah, M. Hanna, D. P. Judge, A. I. Barsdorf, P. Huber, T. A. Patterson, S. Riley, J. Schumacher, M. Stewart, M. B. Sultan, C. Rapezzi, *N. Engl. J. Med.* **2018**, *379*, 1007–1016.
[46] I. Bertini, M. Fragai, C. Luchinat, G. Parigi, *Magn. Reson. Chem.* **2000**, *38*, 543–550.
[47] G. Parigi, E. Ravera, M. Fragai, C. Luchinat, *Prog. Nucl. Magn. Reson. Spectrosc.* **2021**, *124–125*, 85–98.
[48] E. Ravera, G. Parigi, A. Mainz, T. L. Religa, B. Reif, C. Luchinat, *J. Phys. Chem. B* **2013**, *117*, 3548–3553.
[49] J. García de la Torre, M. L. Huertas, B. Carrasco, *J. Magn. Reson.* **2000**, *147*, 138–146.
[50] J. Brunetti, S. Piantini, M. Fragai, S. Scali, G. Cipriani, L. Depau, A. Pini, C. Falciani, S. Menichetti, L. Bracci, *Molecules* **2020**, *25*, E1088.
[51] J. Brunetti, S. Pillozzi, C. Falciani, L. Depau, E. Tenori, S. Scali, L. Lozzi, A. Pini, A. Arcangeli, S. Menichetti, L. Bracci, *Sci. Rep.* **2015**, *5*, 17736.
[52] K. Liu, J. W. Kelly, D. E. Wemmer, *J. Mol. Biol.* **2002**, *320*, 821–832.
[53] J. Oroz, J. H. Kim, B. J. Chang, M. Zweckstetter, *Nat. Struct. Mol. Biol.* **2017**, *24*, 407–413.
[54] B. I. Leach, X. Zhang, J. W. Kelly, H. J. Dyson, P. E. Wright, *Biochemistry* **2018**, *57*, 4421–4430.
[55] Y.-T. Liu, Y.-J. Yen, F. Ricardo, Y. Chang, P.-H. Wu, S.-J. Huang, K.-P. Lin, T.-Y. Yu, *Ann. Clin. Transl. Neurol.* **2019**, *6*, 1961–1970.
[56] A. Corazza, G. Verona, C. A. Waudby, P. P. Mangione, R. Bingham, I. Uings, D. Canetti, P. Nocerino, G. W. Taylor, M. B. Pepys, J. Christodoulou, V. Bellotti, *J. Med. Chem.* **2019**, *62*, 8274–8283.
[57] S. Duhr, D. Braun, *Proc. Natl. Acad. Sci. USA* **2006**, *103*, 19678–19682.
[58] M. Jerabek-Willemsen, C. J. Wienken, D. Braun, P. Baaske, S. Duhr, *Assay Drug Dev. Technol.* **2011**, *9*, 342–353.
[59] S. Grzesiek, A. Bax, G. M. Clore, A. M. Gronenborn, J. S. Hu, J. Kaufman, I. Palmer, S. J. Stahl, P. T. Wingfield, *Nat. Struct. Biol.* **1996**, *3*, 340–345.

Manuscript received: March 13, 2023
Accepted manuscript online: June 5, 2023
Version of record online: ■■, ■■

Research Articles

NMR Spectroscopy

L. Cerofolini, K. Vasa, E. Bianconi, M. Salobehaj, G. Cappelli, A. Bonciani, G. Licciardi, A. Pérez-Ràfols, L. Padilla-Cortés, S. Antonacci, D. Rizzo, E. Ravera, C. Viglianisi, V. Calderone, G. Parigi, C. Luchinat, A. Macchiarulo, S. Menichetti,* M. Fragai* — **e202303202**

Combining Solid-State NMR with Structural and Biophysical Techniques to Design Challenging Protein-Drug Conjugates

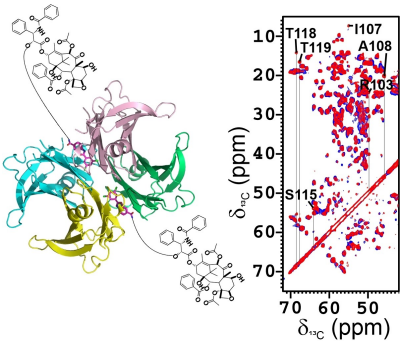

A new molecule that results from the conjugation of the cytotoxic Paclitaxel and Tafamidis, and maintains a high affinity for human transthyretin, demonstrates the potential contribution of solid-state NMR to the structure-based design of novel protein-drug conjugates.